Physica B ■ (■■■■) ■■■–■■■

Contents lists available at ScienceDirect

Physica B

journal homepage: www.elsevier.com/locate/physb

Properties of blue emitting $CaAl_2O_4$:Eu^{2+}, Nd^{3+} phosphor by optimizing the amount of flux and fuel

A.H. Wako [a,*], B.F. Dejene [a], H.C. Swart [b]

[a] Department of Physics, University of the Free State, QwaQwa Campus, Private Bag X13, Phuthaditjhaba 9866, South Africa
[b] Department of Physics, University of the Free State, P.O. Box 339, Bloemfontein 9300, South Africa

ARTICLE INFO

Keywords:
$CaAl_2O_4$:Eu^{2+}, Nd^{3+}
Luminescence
Long afterglow
Eu^{2+}
Nd^{3+}
Doping

ABSTRACT

Long afterglow $CaAl_2O_4$:$0.03Eu^{2+}$, $0.03Nd^{3+}$ phosphor was prepared by solution-combustion synthesis. The active role of boric acid (H_3BO_3) as a flux in enhancing the Eu^{2+} photoluminescence and the effect of a varied amount of urea ($CO(NH_2)_2$) as a fuel on the morphological, structural and photoluminescent (PL) properties of the $CaAl_2O_4$:$0.03Eu^{2+}$, $0.03Nd^{3+}$ systems were investigated. The results of X-ray diffraction, scanning electron microscopy, and PL spectra revealed the influence of the dosage of urea and hence the heated process on the crystallinity, morphology, and luminescence of the phosphor. The addition of H_3BO_3 favoured the formation of a monoclinic $CaAl_2O_4$ phase while the variation of the amount of $CO(NH_2)_2$ showed mixed phases although still predominantly monoclinic. Both H_3BO_3 and $CO(NH_2)_2$ to some extent influence the luminescence intensity of the obtained phosphor but unlike the case of $CO(NH_2)_2$, the presence of H_3BO_3 did not evidently shift the emission peak due to no obvious change in the energy level difference of the 4f–5d levels. The broad blue emissions consisting mainly of symmetrical bands having maxima between 440 and 445 nm originate from the energy transitions between the ground state ($4f^7$) and the excited state ($4f^65d^1$) of the Eu^{2+} ions while the narrow emissions in the red region (600–630 nm) arise from the $^5D_0 \rightarrow {}^7F_2$ transitions of the remnant unreduced Eu^{3+} ions. Higher concentrations of H_3BO_3 (0.228 mol and 0.285 mol) reduce both intensity and lifetime of the phosphor. The optimized content of H_3BO_3 was 0.171 mol for the obtained phosphor with the best optical properties.

1. Introduction

Inorganic materials have practical luminescence applications as artificial light sources in many devices. Rare earth doped aluminates form a group of luminescence materials which exhibit high stability, brightness, and versatile industrial processing characteristics suitable for manufacture of lighting and display devices [1,2], dark vision display devices [3], emergency route markings [4], etc. have been developed. Divalent europium doped $CaAl_2O_4$:$0.03Eu^{2+}$, $0.03Nd^{3+}$ phosphor is well-known for a bluish-green emission with a bright afterglow under UV irradiation [4]. Many research works on phosphors with calcium aluminate as a host have been conducted based on their persistent luminescence and photoconductivity spectrum [5]. The effect of flux on synthesis techniques, structural and luminescent properties has become one of the hotspots in the aluminate luminescent materials activated by rare earth [6–9]. However, the action and mechanism of H_3BO_3 and $CO(NH_2)_2$ in the phosphor are not completely resolved. In this paper, we present the active role of boric acid (H_3BO_3) as a flux and urea ($CO(NH_2)_2$) as a fuel in determining the blue phosphorescence of the $CaAl_2O_4$:$0.03Eu^{2+}$, $0.03Nd^{3+}$ phosphor. H_3BO_3 was chosen in this study as it has very good solubility with the oxide materials employed while urea is commercially readily available, is cheap and generates the highest temperature. Finally, the solution-combustion technique is safe, fast and saves energy. It makes use of the heat energy liberated by the redox exothermic reaction at 500 °C between metal nitrates (oxidizers) and urea (fuel).

2. Experimental details

2.1. Synthesis

$CaAl_2O_4$:$0.03Eu^{2+}$, $0.03Nd^{3+}$ phosphor was synthesized using the solution-combustion method. The starting raw materials used in the experiment included various proportions of analytical pure grade $Ca(NO_3)_2 \cdot 4H_2O$, $Al(NO_3)_3 \cdot 9H_2O$, $Eu(NO_3)_3 \cdot 5H_2O$, $Nd(NO_3)_3$, urea ($CO(NH_2)_2$) and/or boric acid (H_3BO_3). The raw materials were weighed according to the chemical composition of $CaAl_2O_4$:$0.03Eu^{2+}$, $0.03Nd^{3+}$, dissolved in 10 ml of de-ionized water and thoroughly

* Corresponding author. Tel.: +27058 718 5264; fax: +27058 718 5444.
E-mail addresses: wakoah@qwa.ufs.ac.za (A.H. Wako), dejenebf@ufs.ac.za (B.F. Dejene).

0921-4526/$ - see front matter © 2013 Elsevier B.V. All rights reserved.
http://dx.doi.org/10.1016/j.physb.2013.11.047

mixed using a magnetic stirrer for 15 min without heating to obtain a uniform saturated aqueous solution. To investigate the effect of flux, the molar ratio ($Ca(NO_3)_2$:$Al(NO_3)_3$:$Eu(NO_3)_3$:$Nd(NO_3)_3$) of the initial composition was fixed at 1:2:0.03:0.03, to which 0, 0.057, 0.114, 0.171, 0.228 and 0.285 mol of H_3BO_3 were added with respect to the metal ions, with a constant 12.5 mol of $CO(NH_2)_2$ as a fuel. To investigate the effect oxidizer/fuel ratio on the characteristics of the resultant powder, samples were prepared with various urea contents: 2.4, 3.0, 3.6, 6.0, and 10.5 mol of $CO(NH_2)_2$. The solutions were then poured into China crucibles and placed one at a time in a muffle furnace pre-heated at 500 °C. The mixture ignited and a fast, self-sustaining combustion reaction took off. At first, each solution was boiled, losing all the water in the form of steam, followed by decomposition letting off large amounts of gases (oxides of carbon, nitrogen and ammonia). The mixture then frothed and swelled enormously forming foam, then spontaneous ignition and smouldering occurred which gradually led to an explosion which ruptured the foam with a flame that glowed to incandescence. The product of combustion was a voluminous white $CaAl_2O_4$:$0.03Eu^{2+}$, $0.03Nd^{3+}$ foam obtained by combusting the mixture at temperatures of 400–500 °C. The foam was taken out of the muffle furnace, cooled then milled resulting in dry, and usually crystalline, fine white oxide powders. The whole combustion process was over in about 5 min. The powders were stored in transparent glass sample bottles for characterization.

2.2. Characterization

The final structural composition of the $CaAl_2O_4$:$0.03Eu^{2+}$, $0.03Nd^{3+}$ phosphor was determined using a Bruker-AXS D8 Advance X-ray diffractometer (Bruker Corporation of Germany) operating at 40 kV and 4 mA using Cu Kα=0.15406 nm. The morphologies of the phosphor powders were obtained by using a Shimadzu Superscan SSX-550 Scanning Electron Microscope (SEM) coupled with an Energy Dispersive X-ray Spectrometer (EDS) for analysis of elemental composition. Infrared spectra corresponding to the frequencies of vibrations between the bonds of the phosphor atoms were obtained using a Bruker Tensor 27 Fourier Transform Infra-Red (FTIR) spectrometer. The photoluminescence (PL) spectra were recorded at room temperature using a Cary Eclipse luminescence spectrometer (model LS-55) with a built-in 150 W xenon flash lamp as the excitation source and a grating to select a suitable excitation wavelength.

3. Results and discussion

3.1. SEM and EDS analysis

The grain growth and morphological studies along with chemical composition determination was done using SEM coupled with EDS. Fig. 1 shows the representative SEM micrograph taken for (a) 0.057 mol H_3BO_3, (b) 0.114 mol H_3BO_3, (c) 1.5 mol $CO(NH_2)_2$ and (d) 2.4 mol $CO(NH_2)_2$ samples. The samples exhibit irregular morphology as seen from SEM micrographs and so the crystalline phase identification becomes difficult. The calculated average grain sizes for samples in Fig. 1(a) and (b) deduced according to Scherrer's equation using full-width at the half-maximum (FWHM) data [10] of the X-ray diffraction (XRD) patterns are 44 nm. From Fig. 1(b) it can be seen that further addition of boric acid results in smooth grain interfaces with less voids. Fig. 1(c) and (d) shows that urea allows the growth of faceted crystals with clear-cut boundaries. The nanostructures also crystallize to form fine, regular hexagonal platelets exhibiting a smooth surface and well-developed faces as shown in Fig. 1(d). It is well known that phosphors with regular morphology can improve the packing density, slurry properties and the luminescence of phosphors [11]. The EDS spectra of $CaAl_2O_4$:$0.03Eu^{2+}$, $0.03Nd^{3+}$ (Fig. 2(a)) confirms that the nano-phosphors were composed of aluminium, calcium, oxygen, neodymium and europium. Carbon (C) may have come from the tape used to support the sample. Fig. 2(b) shows the FTIR spectra of the samples. The region from ≃1500 to 400 cm^{-1} known as the fingerprint region is characteristic of the molecule as a whole. The absorption bands in the region 420–680 cm^{-1} confirm the presence of a $Ca_3Al_2O_6$, while those at 807 cm^{-1} are from CaA_2lO_4 signals [12]. The asymmetrical stretch of C═O gives a strong band at 2350 cm^{-1} and a degenerate peak appearing at 666 cm^{-1} in the IR spectrum. These signals are due to CO_2 present in the atmosphere. The signals at 1450 cm^{-1} show that high concentrations of H_3BO_3 lead to the formation of borate complexes which reduce transmittance while bands at 3450 cm^{-1} represent the vibration of water bonds [13].

3.2. XRD analysis

Fig. 3(a) and (b) shows the powder XRD patterns of the $CaAl_2O_4$:$0.03Eu^{2+}$, $0.03Nd^{3+}$ phosphor synthesized with H_3BO_3 and $CO(NH_2)_2$ respectively. From Fig. 3(a), it can be observed that the addition of H_3BO_3 facilitated the formation of mainly a single phase with suppression of all the other phases. This is because H_3BO_3 melts at a low temperature and acts as a flux for the synthesis of the phosphor which makes it feasible to obtain single pure phase of $CaAl_2O_4$ [14]. In the absence of H_3BO_3, mixed phases of $CaAl_2O_4$ (JCPDS card no. 70-0134), $Ca_{1.8}Al_2O_{4.8}$ (JCPDS card no. 21-129) and $Ca_3Al_2O_6$ (JCPDS card no. 33-251) were obtained as shown in Fig. 3(b). Analysis of these diffractive peaks reveal that as-prepared $CaAl_2O_4$ powders with $CO(NH_2)_2$ concentrations lower than 6 mol, lead to the formation of other phases as a result of incomplete combustion since the heat was not sufficient to promote the crystallization of the desired phase. However, at 6 mol $CO(NH_2)_2$, $CaAl_2O_4$ became the dominant phase, with only traces of other phases (Fig. 3(b)). This amount of $CO(NH_2)_2$ can be treated as the threshold for the formation of the monoclinic phase for this particular phosphor. This is because the high exothermic temperature due to higher amounts of $CO(NH_2)_2$ resulted in the monoclinic phase with the main diffraction peaks indexing well with the monoclinic structure of $CaAl_2O_4$ according to the card file (JCPDS card no. 70-0134). The line broadening feature in Fig. 3 can be seen due to their smaller grain size, indicating that the phosphor nanocrystallites can be prepared at a far lower temperature (about 500 °C). It is well known that broadening occurs in the diffraction peaks as the grain size of the powders decreases.

3.3. Effect of boric acid

Fig. 4 depicts the effect of H_3BO_3 on the PL spectra of the phosphor. From Fig. 4(a) there is an excitation peak at around 325 nm in the excitation spectrum (λ_{em}=440 nm) which is in conformity with the absorption of the host $CaAl_2O_4$. Also the position of the excitation peaks did not change evidently when the phosphor was synthesized with additional H_3BO_3 except for the 0.171 mol sample that slightly shifted to a lower wave length. Fig. 4(b) represents the emission spectra of Eu^{2+} ion in the $CaAl_2O_4$:$0.03Eu^{2+}$, $0.03Nd^{3+}$ prepared with the various H_3BO_3 concentrations. The UV-excited $CaAl_2O_4$:$0.03Eu^{2+}$, $0.03Nd^{3+}$ phosphor nanoparticles at room temperature yielded high bright blue luminescence peaking at λ_{max}=440 nm. The broadband is symmetric, indicating only one luminescent centre, which is Eu^{2+} luminescent and excitation resulting from transitions between the $4f^65d^1 \rightarrow 4f^7$ electron configurations which gradually increased with increasing H_3BO_3 content. It is well known that it is the flux that facilitates the entry of activator ions into the crystal lattice and aids in the formation of luminescence and traps centres [15]. After attaining a maximum at 0.171 mol, the PL intensity started

Please cite this article as: A.H. Wako, et al., Physica B (2013), http://dx.doi.org/10.1016/j.physb.2013.11.047

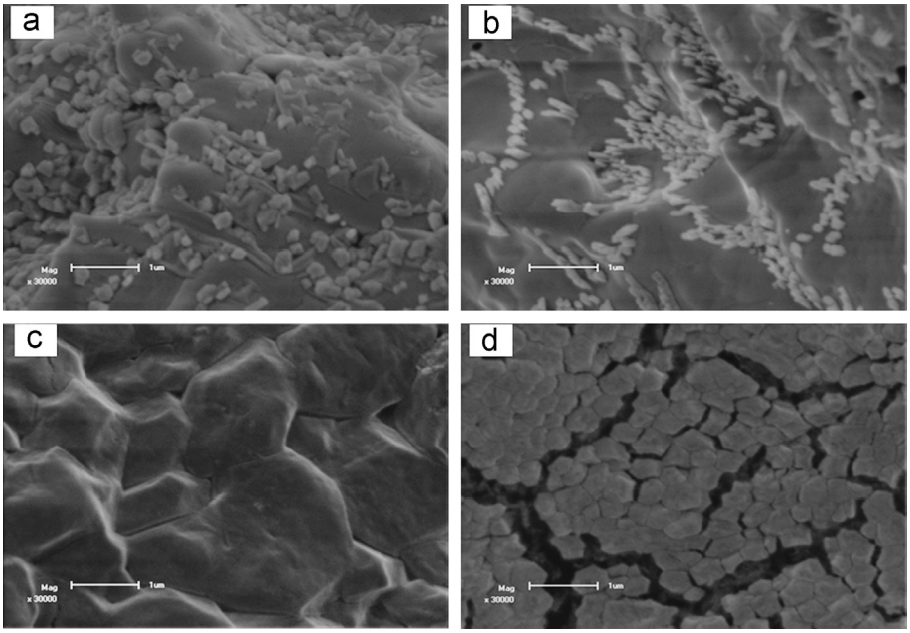

Fig. 1. Sample SEM micrographs for (a) 0.057 mol H_3BO_3 acid, (b) 0.114 mol H_3BO_3 acid, (c) 1.5 mol $CO(NH_2)_2$ and (d) 2.4 mol $CO(NH_2)_2$ all at 6 μm Field of View (FOV).

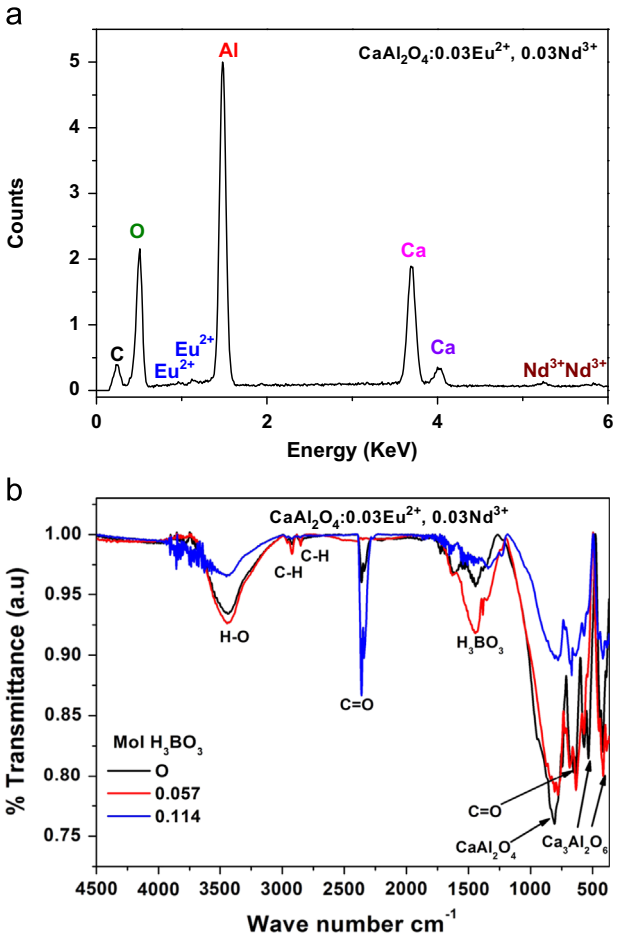

Fig. 2. (a) EDS micrograph revealing the composition of the $CaAl_2O_4$:0.03Eu^{2+}, 0.03Nd^{3+} and (b) FTIR profile showing effect of H_3BO_3 concentration on the $CaAl_2O_4$:0.03Eu^{2+}, 0.03Nd^{3+} molecular bonds.

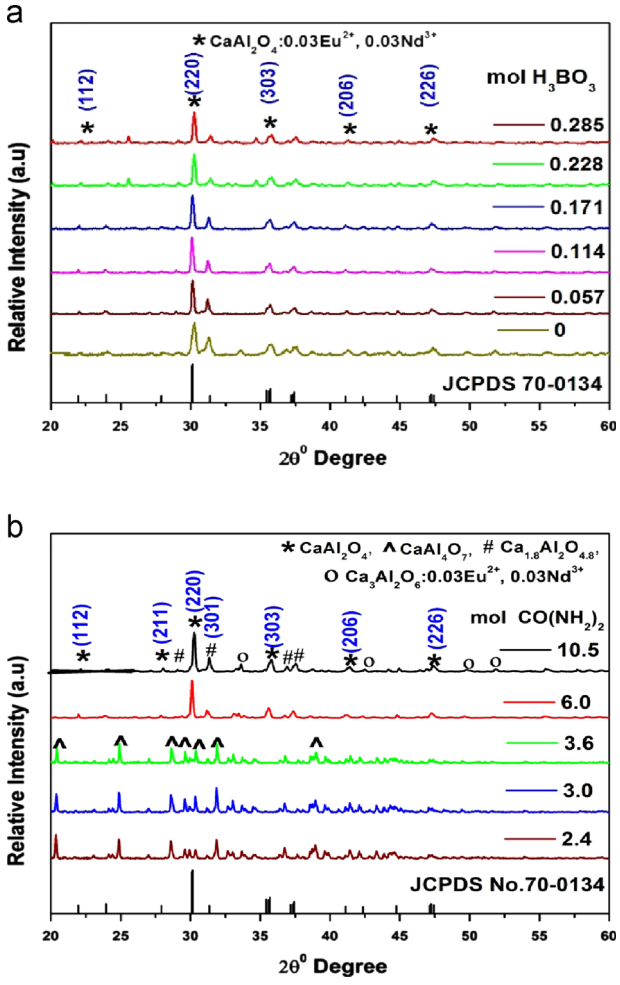

Fig. 3. Effect of (a) amount of H_3BO_3 and (b) $CO(NH_2)_2$ on the structure of the $CaAl_2O_4$:0.03Eu^{2+}, 0.03Nd^{3+} phosphor as compared with JCPDS of monoclinic $CaAl_2O_4$.

decreasing. It also showed some narrow emission peaks in the red region at 614 nm, which is attributed to the transition from $^5D_0 \rightarrow {}^7F_2$ that arise from the remnant unreduced Eu^{3+} ions. Fig. 4(c) shows the effect of different contents of H_3BO_3 on the decay properties of $CaAl_2O_4$:0.03Eu^{2+}, 0.03Nd^{3+}. In the lower (<0.171 mol) concentration range, H_3BO_3 acted as a fluxing agent

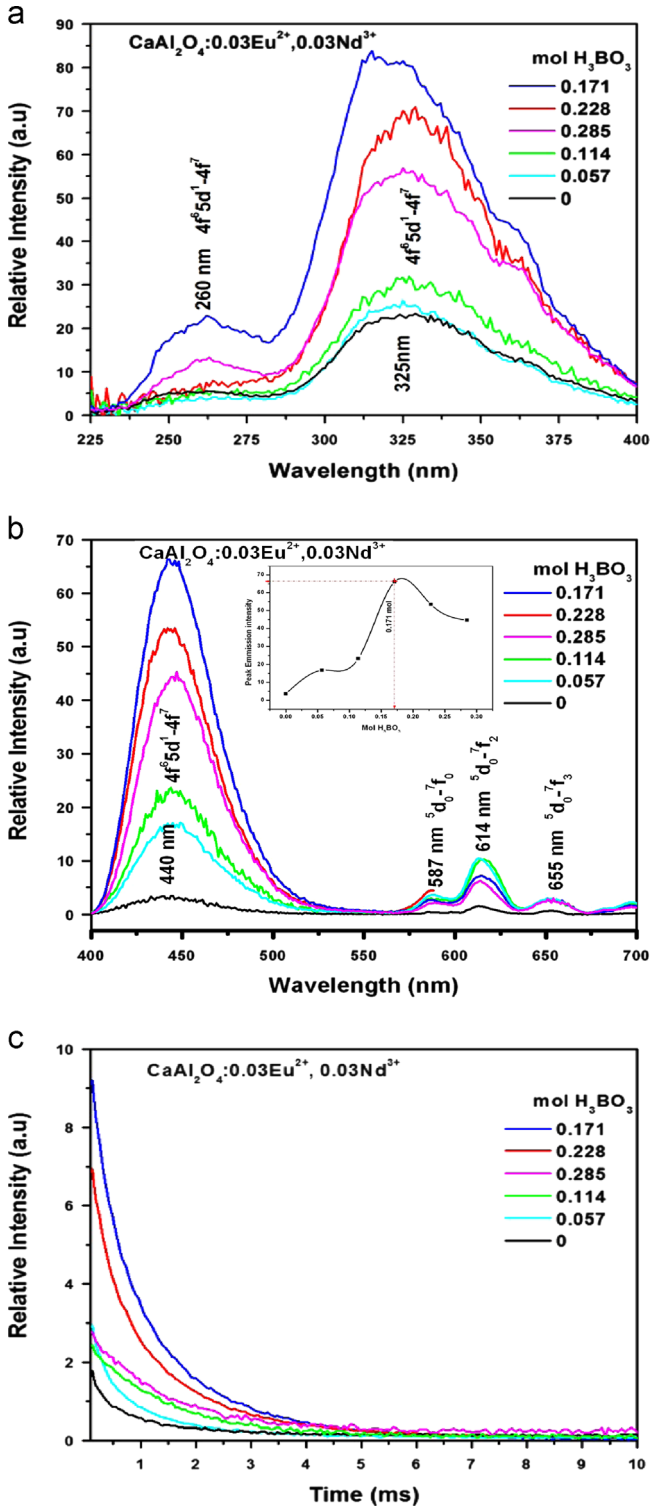

Fig. 4. Effect of the amount of flux (H_3BO_3) on the (a) excitation, (b) emission (inset: intensity vs. mol H_3BO_3) and (c) decay characteristics of the $CaAl_2O_4$:0.03Eu^{2+}, 0.03Nd^{3+} phosphor.

in promoting formation of the required efficient luminescent characteristics culminating at the optimal 0.171 mol, whereas in the higher (>0.171 mol) range it acted as one of the precursors for formation of aluminoborate complexes, which in turn suppressed the luminescence. This supports our argument that the other phases must be contributing to non-radiative transitions [16]. This may be the reason why the 0.228 and 0.285 mol H_3BO_3 showed less PL intensity.

3.4. Effect of urea

As displayed by the spectral characteristics of Fig. 5, it is evident that urea concentration significantly affects PL intensities of the $CaAl_2O_4$:0.03Eu^{2+}, 0.03Nd^{3+} phosphor. As can be seen, a concentration of 10.5 mol urea enhances luminescent properties of the phosphor which is in conformity with previous investigations in which it was suggested that the strongest luminescence in

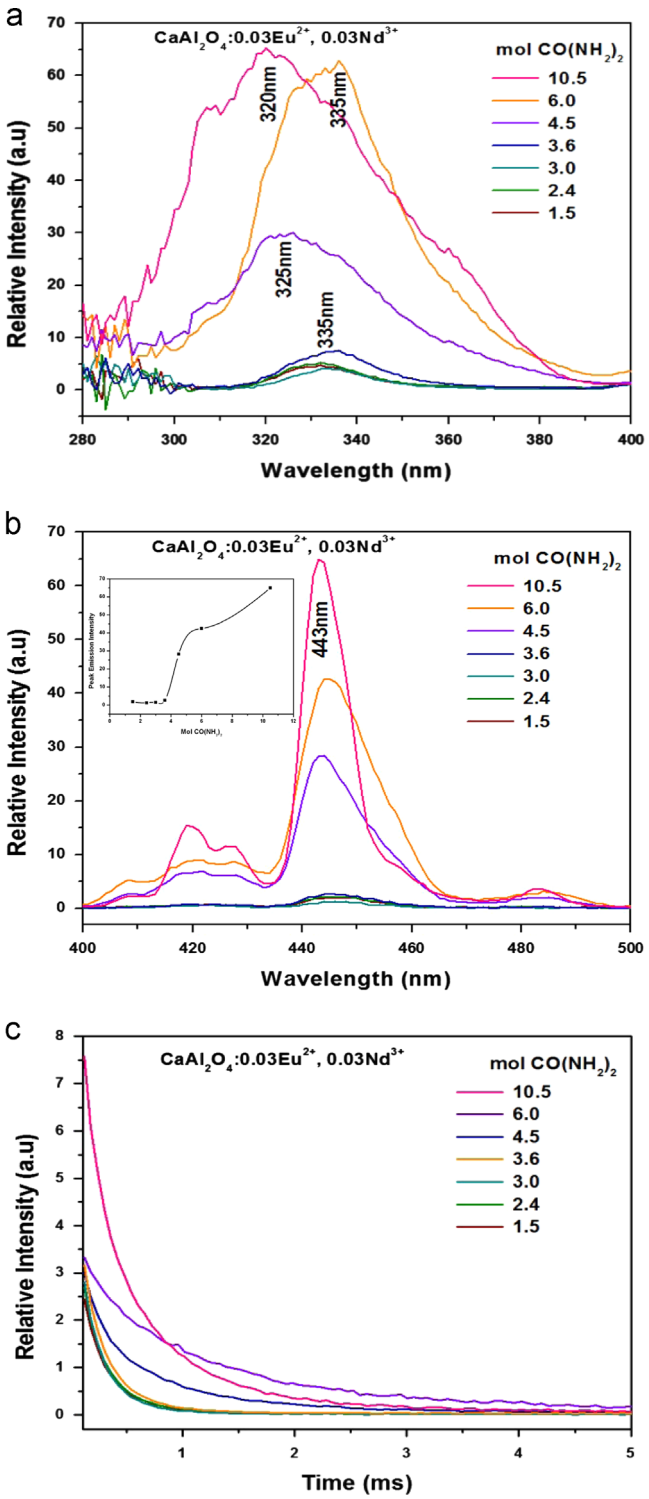

Fig. 5. Effect of the amount of urea ($CO(NH_2)_2$) on the (a) excitation, (b) emission (inset: intensity vs. mol $CO(NH_2)_2$) and (c) decay characteristics of the $CaAl_2O_4$:0.03Eu^{2+}, 0.03Nd^{3+} phosphor.

$CaAl_2O_4$ is obtained for the monoclinic phase [17]. It is also observed that the main peaks of excitation spectra of phosphor nanoparticles shift to shorter wavelength (from 335 to 320 nm). This may result from the changes of the crystal field around Eu^{2+} as the phosphor crystals decrease in size to be nano-sized [18].

4. Conclusions

$CaAl_2O_4$:0.03Eu^{2+}, 0.03Nd^{3+} long persistence phosphor in sub-micrometre scale was prepared by solution-combustion method which is cost-effective, saves energy and time. The influences of the varying quantity of H_3BO_3 and CH_4N_2O on the structural and luminescent properties of the phosphor were studied. The analytical results indicate that the broad emission band of the $CaAl_2O_4$:0.03Eu^{2+}, 0.03Nd^{3+} is observed in the blue region (λ_{max}=440 nm) due to transitions from the $4f^65d^1$ to the $4f^7$ configuration of the Eu^{2+} ion. It is observed that by changing the fuel concentration, one can control particulate and hence the luminescent properties of the phosphor. Flux H_3BO_3 is very crucial and makes it easy to synthesize phosphor powders with desirable characteristics, including very fine size, narrow size distribution, spherically shaped powders, and good chemical homogeneity, leading to the enhancement of luminescent properties. Reaction in the presence of urea allows the growth of faceted crystals since urea acts as a reducing reagent. Liquid interfaces are produced among crystal grains, and then the crystal grains reunite and result in bigger particles. $CaAl_2O_4$:0.03Eu^{2+}, 0.03Nd^{3+} may serve as a promising material for use as a lamp phosphor in the blue region.

Acknowledgements

The authors send immense gratitude to the South Africa's National Research Foundation (NRF) and the Cluster Program of University of the Free State for funding the project and also the University of the Free State Physics and Chemistry Departments for assistance with the research technique systems used to characterize materials for this study.

References

[1] T. Justel, D. Wiechert, J. Lumin. 93 (3) (2001) 179.
[2] L. Zhou, J. Huang, L. Yi, M. Gong, J. Shi, J. Rare Earths 27 (1) (2009) 54.
[3] T. Matsuzawa, Y. Aoki, N. Takeuchi, Y. Murayama, J. Electrochem. Soc. 43 (1996) 2670.
[4] Y. Murayama, S. Shionoya, W. Yen, J. Lumin. 94–95 (2001) 59.
[5] T. Aitasalo, J. Hölsä, H. Jungner, M. Lastusaari, J. Niittykoski, J. Phys. Chem. B 110 (10) (2006) 4589.
[6] J. Niittykoski, T. Aitasalo, J. Hölsä, H. Jungner, M. Lastusaari, M. Parkkinen, M. Tukia, J. Alloys Compd. 374 (2004) 108.
[7] Y. Li, Rare Earth 19 (3) (1998) 68.
[8] N. Wang, D. Wang, Mater. Sci. Eng. 16 (4) (1998) 40.
[9] T.R.N. Abanti Kutty, J. Alloys Compd. 354 (2003) 221.
[10] B. Cullity, Elements of X-ray Diffraction, 2nd ed., Addison-Wesley, Reading, MA (1997) 102.
[11] T. Xiaoming, Z. Weidong, H. Yunsheng, Z. Chunlei, H. Huaqiang, H. Xiaowei, J. Alloys Compd. 458 (2008) 446.
[12] L. Fernández-Carrasco, D. Torrens-Martín, L.M. Morales, S. Martínez-Ramírez, Infrared Spectroscopy in the Analysis of Building and Construction Materials, (2012), ISBN: 978-953-51-0537-4. (Ed.) 370.
[13] F. Miller, C. Wilkins, Anal. Chem. 24 (8) (1952) 1253.
[14] M. Ohring, The Material Science of Thin Films, Academic Press, USA, 1992.
[15] D. Haiyen, L. Gengshen, S. Jaiyue, J. Rare Earths 25 (2007) 19.
[16] G. Blasse, A. Brill A, Philips Tech. Rev. 31 (1970) 303.
[17] T. Aitasalo, H. Hölsä, H. Jungner, M. Lastusaari, J. Niittykoski, Mater. Sci. 20 (2002) 15.
[18] J.S. Kim, J. Ceram. Process. Res. 10 (4) (2009) 443.